Available online at www.sciencedirect.com

SCIENCE DIRECT®

Journal of the European Ceramic Society 25 (2005) 987–995

www.elsevier.com/locate/jeurceramsoc

Phase formation in porous liquid phase sintered silicon carbide: Part I: Interaction between Al_2O_3 and SiC

J. Ihle*, M. Herrmann, J. Adler

Fraunhofer-Institute for Ceramic Technologies and Sintered Materials, Winterbergstr. 28, 01277 Dresden, Germany

Received 10 December 2003; received in revised form 6 April 2004; accepted 22 April 2004
Available online 14 July 2004

Abstract

The structure and phase formation of porous liquid phase sintered silicon carbide (porous LPS-SiC), containing yttria and alumina additives have been studied. The present paper is focused on the system Al–Si–C–O, which is part of the system describing the interactions with sintering additives.

The influence of different sintering atmospheres, namely argon and Ar/CO, and different temperatures on structure and composition was investigated by XRD and SEM. Additionally, reaction products were calculated from thermodynamic data and correlated with experimentally determined reaction products. Alumina and SiC reacted at 1950 °C in an argon atmosphere, forming a metal melt of aluminium and silicon. No reduction of Al_2O_3 was observed in a CO-containing argon sintering atmosphere.

In the second and third parts of this paper the interactions between Y_2O_3–SiC and Y_2O_3–Al_2O_3–SiC are analysed [J. Eur. Ceram. Soc. (in press), parts II and III].

Keywords: SiC; Liquid phase sintering; Phase development; Additives; Al_2O_3

1. Introduction

Silicon carbide is a prevalent ceramic material for many applications in harsh environmental conditions because of its stability at high temperatures, resistance to degradation by aggressive chemicals and abrasion.[3] These are important properties for materials that find application as filters for abrasive suspensions, acids, etc.[4]

The solid phase sintering of SiC (S-SiC) is usually performed at very high temperatures up to 2200 °C with small additions of boron and carbon or boron, aluminium and carbon. In the case of LPS-SiC the additives Al_2O_3 and Y_2O_3 or other rare earth oxide additions form a liquid phase, which accelerates the sintering in comparison with S-SiC. Consequently, the sintering temperature can be reduced to 1800–2000 °C.[3,5–8]

A high degree of open porosity, narrow pore size distribution and an adjustable pore size are an advantage for filters of porous LPS-SiC.[4,9] Fig. 1 shows the structures of porous LPS-SiC.

The sintering process in combination with the resulting liquid phase has a critical influence on structure, phase composition and subsequently the properties of the material. Beside the formation of yttrium–aluminium–garnet (YAG) as intergranular phase between the SiC-grains a reduction of the oxides by the silicon carbide can occur.[6,7,8,10] The properties of LPS-SiC were investigated and published by several authors.[3,7,10–14] Groebner[15] performed a thermodynamic assessment of the Gibbs energy functions for the phases in the system Y–Al–Si–C–O. A complete Gibbs energy data set for the condensed phases was established for thermodynamic calculations in this five-component system.

The decomposition of SiC due to interaction with Al_2O_3 and other oxides such as Y_2O_3 during sintering was analysed by numerous authors.[7,10,11,14,16] A common technique for reducing the decomposition is the implementation of a powder bed. In most cases a mixture of SiC and Al_2O_3 are used for the powder bed.[5,8,12,17]

The major weight-loss during sintering of SiC–Al_2O_3 compositions is mainly caused by the formation of CO, SiO, Al_2O and Al. The gaseous species formed, their

---

* Corresponding author. Tel.: +49 351 2553 682; fax: +49 351 2554 128.
E-mail address: Jan.Ihle@ikts.fraunhofer.de (J. Ihle).

0955-2219/$ – see front matter. © 2004 Elsevier Ltd. All rights reserved.
doi:10.1016/j.jeurceramsoc.2004.04.015

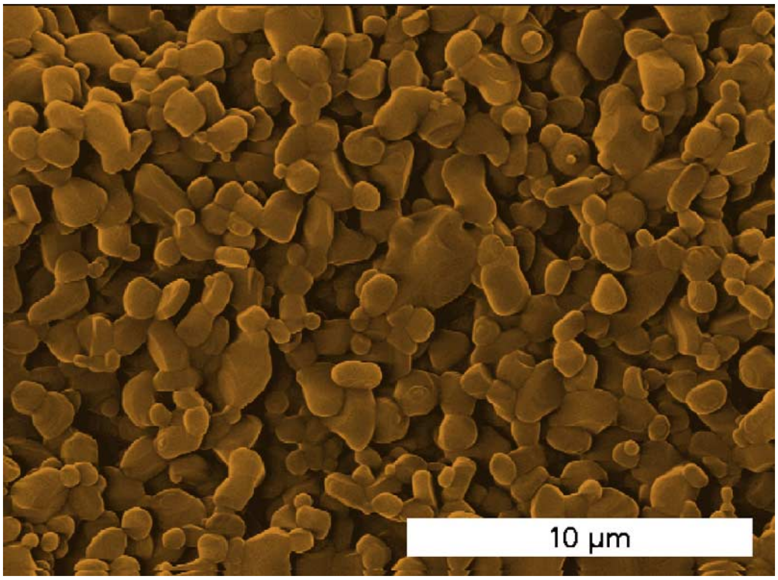

Fig. 1. Micrograph of porous LPS-SiC.

concentration and consequently the extent of weight loss is determined by the sintering atmosphere.[7,10,11,16,18] Based on thermodynamic calculations, the analysis of the interactions of SiC and Al_2O_3 by Misra[19] shows that liquid Al can be formed, in the absence of free carbon, at sintering temperatures in the range of 2223 and 2423 K. The composition of the liquid phase depends on the content of free carbon which also interacts with Al_2O_3 and results in gas formation reactions. Mulla et al.[16] reported that extent of the reaction between SiC and Al_2O_3 during sintering at 2050 °C could be reduced if a pure CO gas atmosphere is used. In this case, the liquid Al–Si alloy formation could be suppressed and the formation of the gaseous reaction products, SiO and Al_2O decreased so that the mass loss was reduced to a quarter of that expected in a non-CO atmosphere.

Baud et al.[10] analyzed the vaporization behaviour of SiC–Al_2O_3 mixtures by thermodynamic calculations and mass spectroscopy in closed and open systems. They detected that a mixture of SiC and Al_2O_3 evaporates congruently up to 2150 K. This is in disagreement with the data of Mulla et al.[16] who suggest an incongruent evaporation with the formation of a Si–Al liquid metal. Using mass spectrometry with a multiple Knudsen cell method, Baud et al.[5,20] identified the gaseous species Al, Al_2O, SiO and CO and measured their relative pressures as a function of alumina content, crucible materials and excess of C or Si. The evaporation and condensation coefficients were also determined. However, Baud et al.[5,20] state, that equilibrium conditions were not reached in all experiments since the vaporization reactions are kinetically hindered. This could be a reason for the discrepancy of the results of Baud et al.[5,10,20] and Mulla et al.[16]

Baud et al.[6] detected that the partial pressures of SiO and CO changed drastically if different SiC powders for the powder bed were used. The oxygen content of the SiC powders and the carbon activity is assumed to be the reason for this behaviour. The measured partial pressures of Al and Al_2O did not change in any appreciable way.[6]

The gas forming reactions are more intensive in the case of porous liquid phase sintered silicon carbide than for dense materials. The high open porosity associated with the large specific surface area, which does not decrease significantly during the sintering process, is the cause for this behaviour. Therefore, the control of the decomposition reactions is much more essential for reproducible material production than in the case of dense materials.

Decomposition and the phase formation in porous LPS-SiC has not been thoroughly investigated and understood. The results for dense materials are not unequivocal. Therefore, model experiments were performed to detect the mechanism of the phase formation and the influence of the oxides Al_2O_3 and Y_2O_3.[1,2] The present paper is a study of the interaction of SiC and Al_2O_3 as a function of temperature and gas atmosphere. The experimental results were discussed on the basis of thermodynamic calculations.

2. Experimental

Samples with a higher content of oxides than original compositions of porous LPS-SiC were produced for a better detection of minor phases and for the improvement of the understanding of phase formation. A composition of 50 wt.% α-SiC (ESK F1200 green) and 50 wt.% Al_2O_3 (Alcoa A16 SG) was chosen. The mixed powders were pressed to tablets with a thickness of 5 mm and a diameter of 25 mm. All samples were sintered in graphite crucibles at 1 bar gas pressure in a graphite heater-furnace. The sintering conditions are shown in Table 1.

Table 1
Sintering temperatures, dwell time, atmospheres and phase compositions

Temperature (°C)	Dwell time (h)	Atmosphere	Phase composition of sintered samples
1850	1	Argon	α-SiC, Al_2O_3
1925	1	Argon	α-SiC, Si, Al, Al_2O_3
1925	1	Argon + CO	α-SiC, Al_2O_3
1950	1	Argon	α-SiC, Si, Al

Graphite foil was placed between the crucibles and the samples to prevent a bonding of samples to the crucible by the formation of liquids during sintering. It was not possible to measure exactly the mass loss because some graphite foil remained bonded to the samples after sintering. No mass loss results are therefore presented.

The phase composition of the samples was determined by X-ray diffraction analysis (XRD 7; Seifert-FPM; Cu Kα) and using JCPDS standards.[21] Rietveld analysis (AutoQuan software) was used for the quantitative determination of the phase composition from XRD measurements.

The analysis of the microstructure of polished surfaces of the materials was performed using optical and scanning electron microscopy with attached EDX (Leica Stereoscan 260).

The FactSage® software package was used for thermodynamic calculations[22] and the partial pressure of gas phases and phase formation in the system Al–Si–O–C–Ar were calculated. The necessary thermodynamic data for calculations were taken from the SGTE (Scientific Group Thermodata Europe) pure substance database (SGPS)[23] and solution database (SGSL)[24] as well as the special data set of the system Y–Al–Si–C–O from SGTE[25] based on the data set of Groebner.[15] The data for the Al_4O_4C phase were taken from Lihrmann et al.[26] in accordance with Qiu et al.[27] and Yokokawa et al.[28] For the metallic melt the RKMP model (Redlich–Kister–Muggiano polynomial) from the special data set of the system Y–Al–Si–C–O[25] was used.

3. Results and discussion

3.1. Thermodynamic calculations

Preliminary calculations, using the SGTE database,[23] suggest the presence of Al_4O_4C in addition to Al_2O_3 and SiC. The evaluation of this data shows, that ΔG° (2200 K) for the reaction

$$4Al_2O_3 + Al_4C_3 \leftrightarrow 3Al_4O_4C \qquad (1)$$

is −122 kJ/mol. Also, the data from different phase studies[26–28] show that Al_4O_4C is not stable at temperatures above 1870 °C (2143 K) and has to decompose to Al_2OC and an oxide rich melt. We have therefore taken the thermodynamic data for Al_4O_4C from the original literature source.[26] Using this data we find a much lower ΔG° (2200 K) for reaction (1) of −35 kJ/mol and consequently this phase was no longer present in the calculated equilibrium composition.

The calculations result in different compositions depending on the C and CO activities or the amount of argon used in the calculations. Table 2 shows some of the results. The effective amount of free carbon and the effective volume in the sintering experiments can not be properly predicted, due to different transport reactions, temperature gradients and so on. Therefore, for the interpretation of the results it is necessary to take into account the Gibbs' phase rule

$$F = C - P + 2 \qquad (2)$$

with F, degrees of freedom, C, number of components (in our system 5), P, number of phases in the equilibrium.

Table 2
Results of thermodynamic calculations (2.5 mol SiC + 1.0 mol Al_2O_3) with different additional amounts of carbon and different amounts of argon in calculations at 2223 K (1950 °C)

Phases	C = 0.001 mol			C = 1 mol			CO = 0.1 mol		
	Ar = 0.1 mol	Ar = 1 mol	Ar = 10 mol	Ar = 0.1 mol	Ar = 1 mol	Ar = 10 mol	Ar = 0.1 mol	Ar = 1 mol	Ar = 10 mol
SiC (mol)	2.465	2.140	0.244	2.447	2.384	1.131	2.492	2.238	0.267
Al_2O_3 (mol)	0.984	0.841	–	0.883	0.691	–	0.994	0.874	–
C (mol)	–	–	–	0.536	–	–	–	–	–
Al_4SiC_4 (mol)	–	–	–	0.047	0.083	–	–	–	–
Liquid metal (mol)	0.049	0.502	3.085	–	0.014	2.175	–	0.334	3.026
Al (mol fraction)	0.445	0.441	0.436	–	0.682	0.518	–	0.451	0.437
Al (activity)	0.338	0.334	0.329	–	0.614	0.420	–	0.344	0.330
C (mol fraction)	0.012	0.012	0.012	–	0.054	0.018	–	0.012	0.012
C (activity)	0.009	0.009	0.009	–	0.023	0.011	–	0.009	0.009
Si (mol fraction)	0.543	0.547	0.552	–	0.264	0.464	–	0.537	0.551
Si (activity)	0.490	0.495	0.501	–	0.197	0.395	–	0.482	0.499
Ar (mbar)	666.1	666.1	757.8	217.2	504.5	754.7	450.2	665.9	751.9
CO (mbar)	237.2	236.7	168.3	711.6	396.3	175.9	482.3	238.0	172.7
SiO (mbar)	55.8	56.9	41.5	12.4	15.1	27.0	32.0	54.4	42.3
Al_2O (mbar)	25.5	25.1	17.5	38.3	56.5	23.5	21.9	26.1	18.1
Al (mbar)	15.1	14.9	14.6	20.4	27.4	18.7	13.5	15.3	14.7

For a stable result of the calculation, i.e. no change in the composition of the gas phase with changing starting composition, the degrees of freedom must be 2 (one degree of freedom is connected with a free change of temperature and one degree with the free change of the overall pressure, which was taken as 0.1 MPa). If only two condensed phases Al_2O_3 and SiC exists beside the gas phase, than the degrees of freedom in the system becomes 4. This means that for a given temperature and overall pressure the gas phase has two degrees of freedom, i.e. even small changes in the starting composition changes the composition of the gas phase. In the calculation (Table 2) an additional liquid metallic phase with a large area of homogeneity was observed under different conditions. Therefore, a given composition of the liquid metallic phase in equilibrium with Al_2O_3 and SiC will result in a fixed composition of the gas phase. The composition and amount of the liquid metal change with increasing amount of carbon in the system.

The amounts of elements used for the thermodynamic calculations were 2.0 mol aluminium, 3.0 mol oxygen, 2.5 mol silicon, 2.3, ..., 3.0 mol carbon in steps of 0.1 and 1 mol argon. This corresponds to a composition of 1.0 mol Al_2O_3 and 2.5 mol non-stoichiometric $SiC_{(x)}$ with a range of a deficit of carbon up to −0.2 mol (e.g. 2.3 SiC mol and 0.2 mol free silicon) for the low carbon content and an additional carbon content of 0.5 mol for the high carbon content.

The existence of a liquid metal Al–Si with some C solved in it was indicated under these conditions in a temperature range of 1700–2250 K depending on the amount of additional carbon (Fig. 2). Baud et al.[10] calculated a liquid metal at temperatures higher than 2150 K. Mulla et al.[16] described the formation of liquid Al–Si alloy at 2323 K. The calculations show that these different temperatures of formation depend mostly on the gas volume, the carbon and the CO content of the starting composition (Fig. 2).

The calculations (Fig. 3) show that the main gas species of the system at temperatures between 1950 and 2250 K are Ar, CO, SiO, Al_2O and Al. All other gas species have a partial pressure which is several orders of magnitude lower (Fig. 3). Gaseous Al has a pressure less than half of the pressure of Al_2O at high temperatures and in presence of the liquid metal. At low temperatures the Al pressure is of

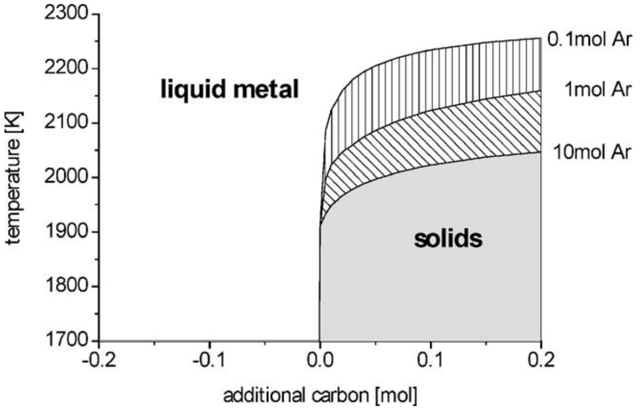

Fig. 2. Calculated stability area of liquid metal phase as a function of carbon and argon content in the system (composition: 2.5 mol SiC, 1 mol Al_2O_3, −0.2, ..., 0.2 mol additional carbon and different amount of argon).

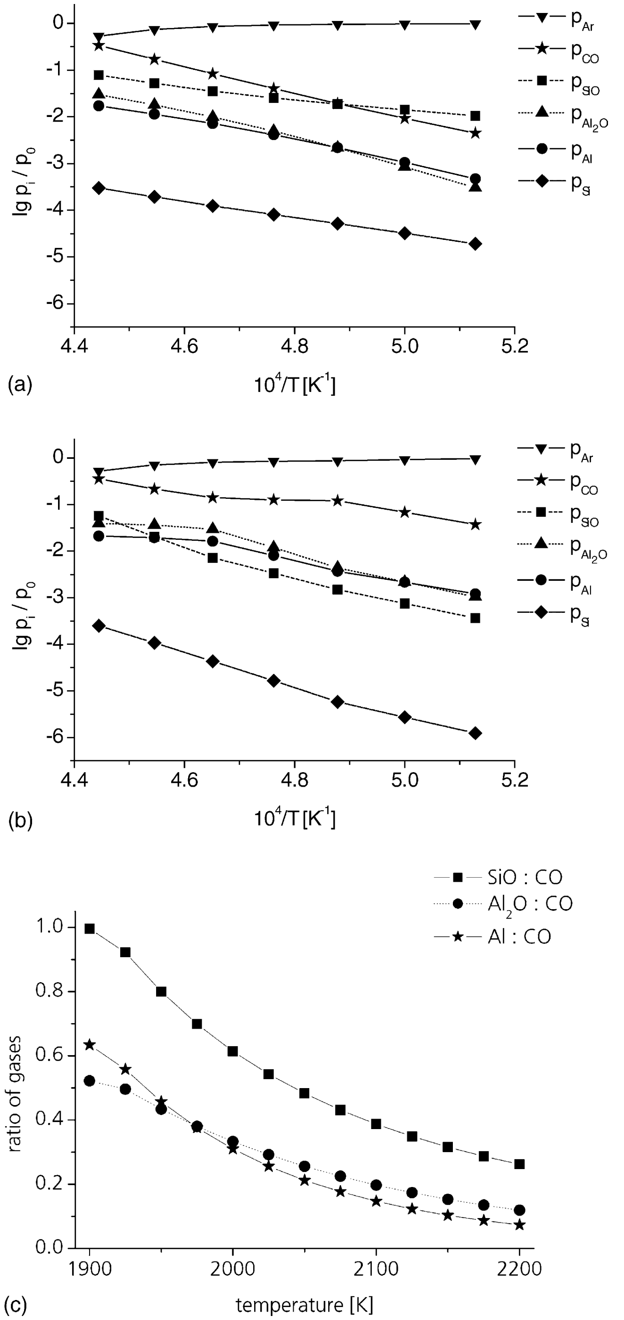

Fig. 3. Calculated partial pressures of gas species of the system Si–C–Al–O–Ar as a function of the inverse temperature ($p_0 = 0.1$ MPa). (a) Results of calculations with deficit of −0.05 mol carbon (condensed phases SiC, Al_2O_3, liquid metal). (b) Results of calculations with 0.2 mol added carbon (condensed phases SiC, Al_2O_3, liquid metal for $10^4/T \leq 4.61\ K^{-1}$; SiC, Al_2O_3, Al_4SiC_4, liquid metal for $10^4/T \leq 4.65\ K^{-1}$; SiC, Al_2O_3, Al_4SiC_4 for $10^4/T \leq 4.88\ K^{-1}$, above SiC, Al_2O_3, C, Al_4SiC_4). (c) Calculated ratio of the partial pressures p_{SiO}/p_{CO}, p_{Al_2O}/p_{CO} and p_{Al}/p_{CO} as a function of temperature (calculations without added carbon).

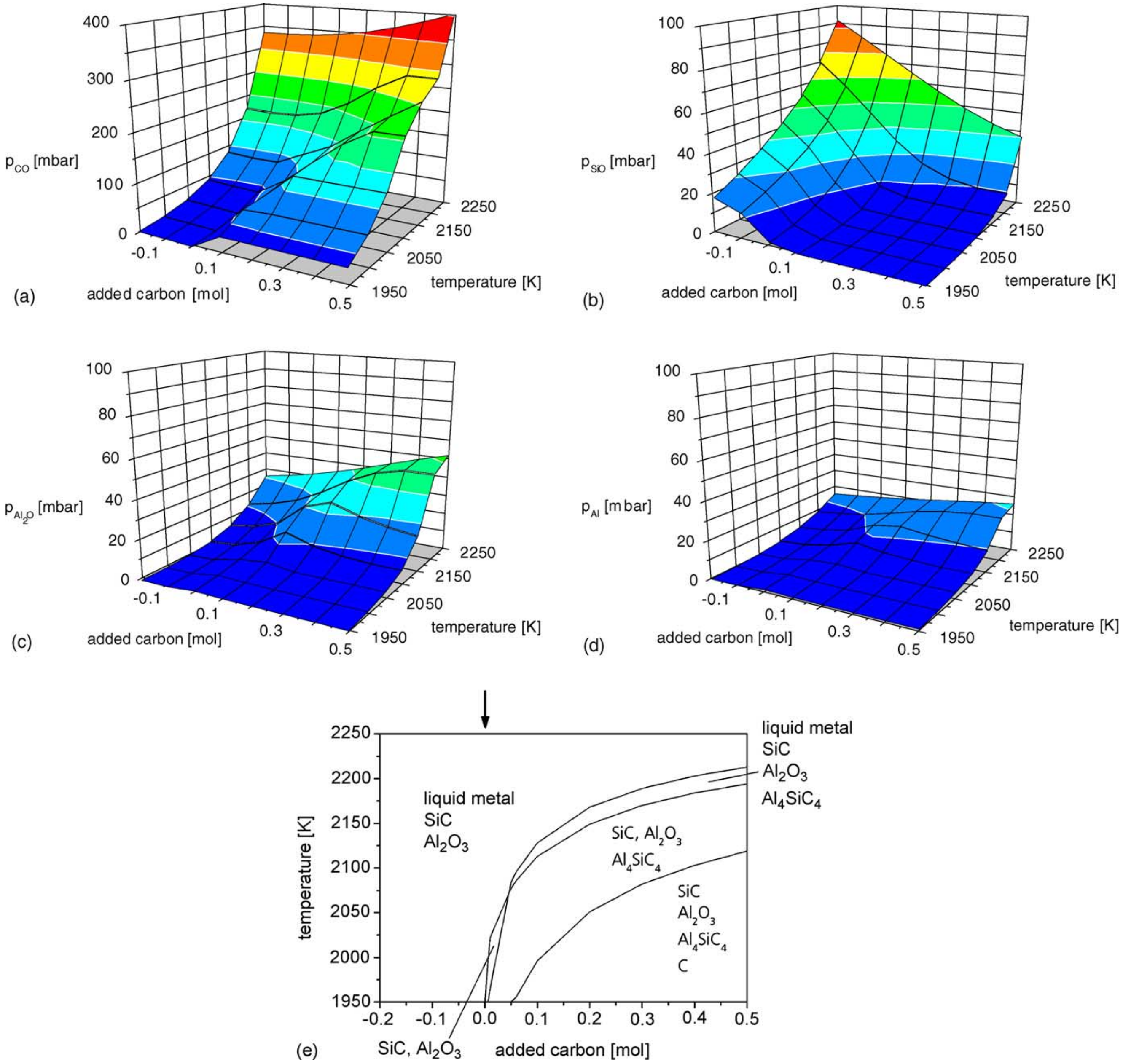

Fig. 4. Results of thermodynamic calculations of partial pressure of CO (a), SiO (b), Al_2O (c) and Al (d) as a function of carbon content and temperature and formed condensed phases (e). The arrow marks the stoichiometric composition Al_2O_3–SiC.

the same order of magnitude or even higher than the Al_2O pressure.

The partial pressures of CO, SiO, Al_2O and Al as a function of carbon content and temperature are plotted in Fig. 4. The calculated partial pressure of SiO is higher than the partial pressure of CO up to a temperature of 2050 K for a deficit of carbon, but is much lower than the CO partial pressure if a higher carbon activity is assumed (Fig. 4). For the composition without additional carbon the ratio p_{SiO}/p_{CO} is less than 0.5 for temperatures higher 2100 K (Fig. 3c). The partial pressure of Al_2O is lower than the SiO partial pressure. With increasing carbon content the partial pressure of Al_2O rises and the partial pressure of SiO decreases. The concentrations of Al and Si in the metal melt vary in the same way. The partial pressure of CO at 2200 K is 172 mbar with a deficit of −0.2 mol carbon and 287 mbar with 0.5 mol additional carbon. The different carbon content also results in different compositions of the liquid metal (Table 3).

Baud et al.[10] calculated a partial pressure of $Al_{(g)}$ 100 times lower than the gaseous species CO, SiO and Al_2O for a closed system under vacuum. In the open system calculations by Baud et al.[10] the partial pressure of $Al_{(g)}$ is much higher than that of Al_2O and the partial pressure of CO is smaller than that of SiO. The reason for these differences may be due to the Knudsen conditions of the calculations by Baud et al.,[10] without taking into account the liquid Si–Al melt.

Table 3
Compositions of the calculated liquid metal C–Al–Si at 2200 K in comparison to the experimentally determined Si:Al ratio after sintering at 2198 K (1925 °C)

Components	Mol fraction of components			
	Calculations without added C	Calculations with 0.2 mol C	Calculations with 0.5 mol C	Sintered samples
Carbon	0.010	0.025	0.047	–
Aluminium	0.443	0.599	0.685	0.60 ± 0.05
Silicon	0.546	0.376	0.268	0.40 ± 0.04

On the basis of our calculations, the net interaction reaction taking place in argon atmosphere at 1 bar can be simply written as:

$$5SiC_{(s)} + 3Al_2O_{3(s)} \rightarrow 5CO_{(g)} + 2Si_{(melt)} + 3Al_{(melt)} + 3SiO_{(g)} + Al_2O_{(g)} + Al_{(g)} \qquad (3)$$

Whereas Al and Si form a single metallic melt. This confirms the calculations of Mulla et al.[16] The partial pressure of gaseous aluminium and Al_2O is directly correlated with the activity (concentration) of Al in the melt, i.e. with increasing carbon content in the system the Al content in the metal melt increases and therefore the Al and Al_2O partial pressure increases too. For lower temperatures the weight loss due to evaporation as Al can be similar to the losses due to Al_2O evaporation, while at higher temperatures ($\geq$2000 K) the evaporation as Al is less than that in form of Al_2O.

Eq. (3) has to be interpreted in the following manner:

If the CO, SiO, Al_2O or Al partial pressures are higher than the equilibrium pressure of the Eq. (3) (see Figs. 3 and 4) than the reaction is shifted to the left side, i.e. the decomposition is reduced. In the extreme case the occurrence of a liquid metal can be prevented. Only when one of the condensed phases disappears, e.g. the liquid metal or Al_2O_3 the partial pressures of the components are no longer fixed and can therefore increase (CO, SiO, Al_2O and $Al_{(g)}$).

From the results of the calculations it was apparent that the composition could be modified with different atmospheres consisting of argon and CO in different mixtures (Table 2; Fig. 4). The formation of liquid metal is shifted to higher temperatures or even eliminated with an increase of admixture of CO. In an argon atmosphere there is a mixture of SiC–Al_2O_3 at 1850 K, which changes to SiC–Al_2O_3 liquid metal at 1912 K. With a given partial pressure of 300 mbar CO the mixture at 1850 K consisting of SiC–Al_2O_3–C changes to SiC–Al_2O_3 at 2083 K and to SiC–Al_2O_3 liquid metal at 2238 K. If a partial pressure of 400 mbar CO is used in the calculations, the composition will change from SiC–Al_2O_3–C to SiC–Al_2O_3 at 2110 K. No liquid metal formation is indicated under these conditions and by further calculations at higher given CO pressures.

The calculations have shown that the decomposition can be minimized effectively by controlling the CO pressure. If the CO pressure is higher than that observed for the equilibrium (3) (Fig. 4a), e.g. more than 0.03–0.04 MPa at 2250 K, depending on the carbon activity (Fig. 4a), the formation of liquid metal can be prevented (see Table 2). These conclusions were verified experimentally.

In the thermodynamic calculations the SiO_2 existing on the surface of the SiC-starting powder was not taken into account. From previous investigations it is known that it evaporates nearly completely between 1750 and 1950 K, i.e. below the temperature range considered in the calculations discussed here.

3.2. Experimental determination of the interaction

Sintering was performed under conditions normally used for sintering of LPS-SiC with the exception of a higher additive content to investigate the relevant phase formation

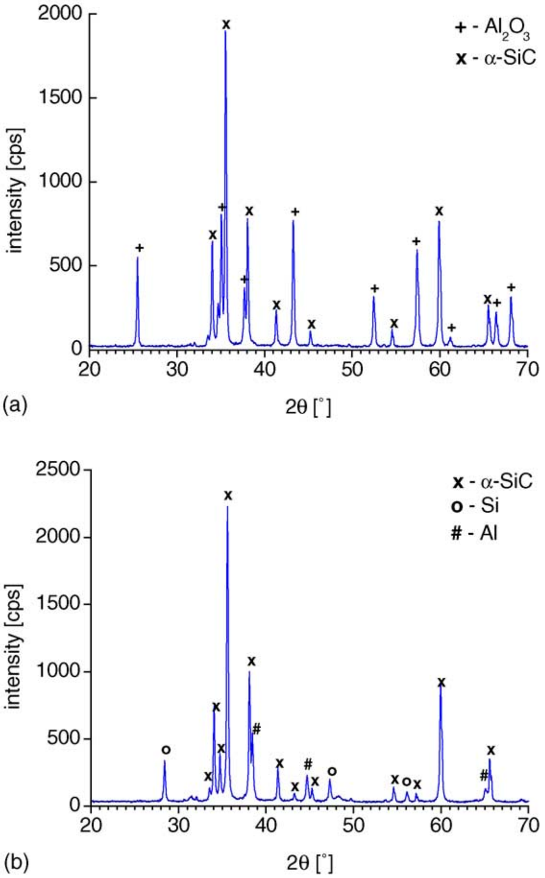

Fig. 5. Results of X-ray diffraction analysis of samples sintered in argon at 1850 °C (a) and 1950 °C (b).

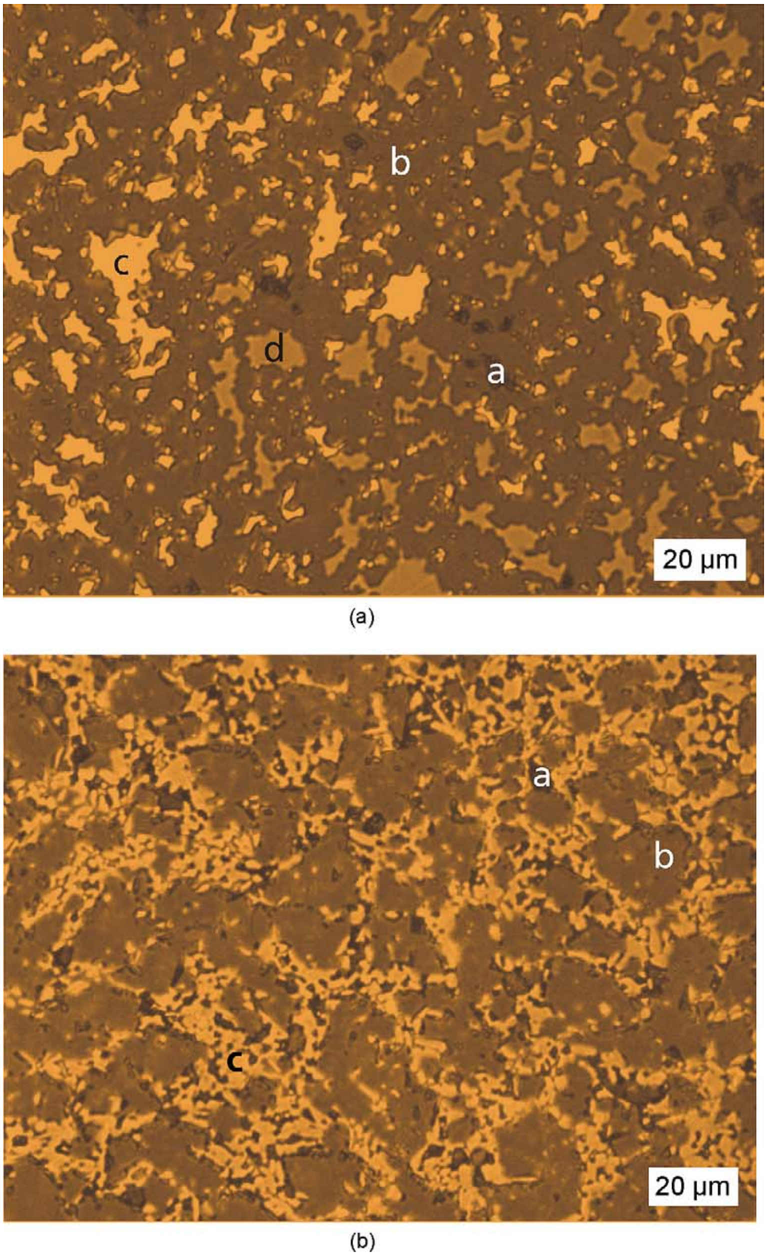

Fig. 6. Optical micrographs of sintered samples. (a) Sample sintered in pure argon atmosphere (marked areas are: a, pore; b, SiC; c, Al; d, Si); (b) Sample sintered in Ar/CO atmosphere (marked areas are: a, pore; b, SiC; c, Al_2O_3).

of porous LPS-SiC. The model experiments reveal that the final composition of the samples sintered at various temperatures strongly depends on sintering conditions (Table 1). After sintering at 1850 °C no change of phase composition in comparison with the initial composition was observed by XRD (Fig. 5a), whereas after sintering at 1950 °C in pure argon the XRD analysis showed that the material consisted of SiC and silicon and aluminium (Fig. 5b). SEM and EDX investigations support this result (Fig. 6). The material exhibited regions of nearly pure silicon and pure aluminium solidifying from the melt in separate phases during the cooling at the end of the sintering. This is in agreement with the Si–Al phase diagram.[29] The morphology of SiC grains in the sample indicates their grain growth.

Samples sintered at 1925 °C (2198 K) in argon atmosphere contain SiC, alumina and elemental silicon and aluminium. The different compositions at various temperatures are caused by an alteration of the reaction kinetics. It may be expected that a longer dwell time at 1850 and 1925 °C results in more complete reduction, if the same furnace is used. If the ratio of sample volume to the volume of the crucible or furnace is low, thermodynamic equilibrium of the composition of the gas phase is not reached. Therefore, the reaction does not stop before the complete alumina is decomposed.

The sintered samples at 1950 °C (2223 K) contained only SiC in addition to silicon and aluminium.

Table 3 shows the Si:Al ratio in the materials sintered at 1925 °C (2198 K) in Ar quantified by Rietveld analysis from the XRD measurement in comparison to the thermodynamically calculated composition of the liquid metal C–Al–Si at 2200 K. The thermodynamically calculated amounts were similar to the experimentally observed values indicating an effective additional carbon content of 0.2 mol under experimental conditions. Also, no Al_4O_4C was detected under all sintering conditions, which is in agreement with the calculations based on the modified data for Al_4O_4C.

The area of the graphite foil, which was used to prevent a bonding of samples to the crucibles, that was in contact with the sample during sintering at 1925 °C had a metallic orange discolouration. The XRD analysis of this phase indicated a composition of Al_4SiC_4, the presence of which was confirmed by thermodynamic calculations (Table 2; Fig. 4e).

With regard to the thermodynamic calculations, sintering experiments were performed in an atmosphere containing CO. The calculated CO partial pressure necessary for stabilising SiC and Al_2O_3 was applied, and the results show that a stabilization of SiC and Al_2O_3 is achieved. The micrographs of the samples show clearly that samples sintered under an Ar/CO atmosphere have a different structure to that of samples sintered under pure argon (Fig. 6). They consist only of SiC and Al_2O_3. Also, by an analysis of the cross section, no elemental silicon and aluminium were observed, which was confirmed by XRD results.

4. Conclusions

Model experiments for the decomposition of mixtures of SiC–Al_2O_3 were carried out at 1850–1950 °C (2123–2223 K) in different atmospheres. The results were compared with thermodynamic calculated ones. They can be summarised as follows.

After sintering in argon at 1950 °C (2223 K), materials with a composition of 50 wt.% SiC and 50 wt.% Al_2O_3 contain, in addition to SiC, a metallic melt consisting of silicon and aluminium. Sintering at 1925 °C (2198 K), with dwell time of 1 h, results in a material with a composition of SiC, an aluminium–silicon melt and some residual Al_2O_3. The phase composition of samples sintered at 1850 °C (2123 K) in argon showed no significant change compared to the initial composition, indicating the low rate of decomposition at these temperatures. Thermodynamic calculations, however, reveal that metal melt can also be formed at lower temperatures. The absence of the metal in experiments at lower temperatures seems to be connected with the lower partial pressures, lower reaction rates and carbon content in the system.

Thermodynamic calculations confirmed the experimental results. The main gaseous species formed by the decomposition of Al_2O_3–SiC mixtures are CO, SiO, Al_2O and Al. The CO partial pressure at normal sintering temperatures is at least three times higher than that for the other species and depends only weakly on the carbon content.

The reaction between SiC and Al_2O_3 during sintering can be successfully suppressed if an Ar/CO atmosphere is used. The materials sintered at 1950 °C in such an atmosphere show no significant change in the phase composition. No metallic silicon or aluminium are formed which is confirmed by X-ray diffraction results and SEM analysis of the microstructure.

References

1. Ihle, J., Herrmann, M. and Adler, J., Phase formation in porous liquid phase sintered silicon carbide: II. Interaction between Y_2O_3 and SiC. *J. Eur. Ceram. Soc.* 2005, **25**, 997–1003.
2. Ihle, J., Herrmann, M. and Adler, J., Phase formation in porous liquid phase sintered silicon carbide: III. Interaction between Al_2O_3–Y_2O_3 and SiC. *J. Eur. Ceram. Soc.* 2005, **25**, 1005–1013.
3. Schwetz, K. A., Silicon carbide based hard materials. *Handbook of Ceramic Hard Materials*, ed. R. Riedel. Wiley-VCH, Germany, 2000.
4. Adler, J., Klose, T. and Piwonski, M., SiC ceramics with pore sizes from nanometers to micrometers. *Materials Week 1998, Band III*. Wiley-VCH, Germany, 1999, pp. 287–292.
5. Baud, S., Thévenot, F. and Chatillon, C., High temperature sintering of SiC with oxide additives: II. Vaporization processes in powder beds and gas-phase analysis by mass spectrometry. *J. Eur. Ceram. Soc.* 2003, **23**, 9–18.
6. Baud, S., Thévenot, F. and Chatillon, C., High temperature sintering of SiC with oxide additives: IV. Powder beds and the influence of vaporization on the behaviour of SiC compacts. *J. Eur. Ceram. Soc.* 2003, **23**, 29–36.
7. Grande, T., Sommerset, H., Hagen, E., Wiik, K. and Einarsrud, M.-A., Effect of weight loss on liquid-phase-sintered silicon carbide. *J. Am. Ceram. Soc.* 1997, **80**(4), 1047–1052.
8. Pujar, V. V., Jensen, R. P. and Padture, N. P., Densification of liquid-phase-sintered silicon carbide. *J. Mater. Sci. Lett.* 2000, **19**, 1011–1014.
9. Schubert, C., Adler, J., Schulz, I. and Klose, T., Ceramic membranes with high physical and chemical stability based on SiC and Si_3N_4. *Conference on "Materials Research under Environmental Aspects", Dresden 1994, Environmental Aspects in Materials Research*. Warlington, 1994, p. 283.
10. Baud, S., Thévenot, F., Pisch, A. and Chatillon, C., High temperature sintering of SiC with oxide additives: I. Analysis in the SiC–Al_2O_3 and SiC–Al_2O_3–Y_2O_3 systems. *J. Eur. Ceram. Soc.* 2003, **23**, 1–8.
11. Schuesselbauer, E., Adler, J., Jaenicke-Roeßler, K. and Leitner, G., Sintering investigations on LPS-SiC. *Werkstoffwoche 98, Band VII*. 1999, pp. 207–212.
12. Cordrey, L., Niesz, D. E. and Shanefield, D. J., *Sintering of Silicon Carbide with Rare-Earth Oxide Additions, Sintering of Advanced Ceramics*, ed. C. A. Handwerker, J. E. Blendell and W. Kayser. The American Ceramic Society, Inc, Westerville, OH, 1990, pp. 618–636.
13. Gadalla, A., Almasry, M. and Kongkachuichay, P., High temperature reactions within SiC–Al_2O_3 composites. *J. Mater. Res.* 1992, **7**(9), 2585–2592.
14. Samanta, A. K., Dharguupta, K. K. and Ghatak, S., Decomposition reactions in the SiC–Al–Y–O system during gas pressure sintering. *Ceram. Int.* 2001, **27**, 123–133.

15. Groebner, J., *Constitution Calculations in the System Y–Al–Si–C–O*. Ph.D. thesis, University of Stuttgart, Germany, 1994.
16. Mulla, M. A., Krstic, V. D. and Thompson, W. T., Reaction-inhibition during sintering of SiC with Al_2O_3 additions. *Can. Metallurg. Q.* 1995, **34**(4), 357–362.
17. Winn, E. J. and Clegg, W. J., Role of the powder bed in the densification of silicon carbide sintered with yttria and alumina additives. *J. Am. Ceram. Soc.* 1999, **82**(12), 3466–3470.
18. Nagano, T., Kaneko, K., Zhan, G.-D. and Mitomo, M., Effect of atmosphere on weight loss in sintered silicon carbide during heat treatment. *J. Am. Ceram. Soc.* 2000, **83**(11), 2781–2787.
19. Misra, A. K., Thermochemical analysis of the silicon-carbide-alumina reaction with reference to liquid phase sintering of silicon carbide. *J. Am. Ceram. Soc.* 1991, **74**(2), 345–351.
20. Baud, S., Thévenot, F. and Chatillon, C., High temperature sintering of SiC with oxide additives: III. Quantitative vaporization of SiC–Al_2O_3 powder beds as revealed by mass spectrometry. *J. Eur. Ceram. Soc.* 2003, **23**, 19–27.
21. Joint Committee on Powder Diffraction Standards, ASTM, Swartmore, 2001.
22. Bale, C. W., Chartrand, P., Degterov, S. A., Eriksson, G., Hack, K., Ben Mahfoud, R. *et al.*, FactSage thermochemical software and databases. *Calphad* 2002, **26**(2), 189–228.
23. *SGPS—SGTE Pure Substances Database*. Scientific Group Thermodata, Europe, 2000.
24. *SGSL—SGTE Alloy Solutions Database*. Scientific Group Thermodata, Europe, 1998.
25. *9288A00S—SGTE Si–Y–Al–C–O Database*. Scientific Group Thermodata, Europe, 2000.
26. Lihrmann, J.-M., Tirlocq, J., Descamps, P. and Cambier, F., Thermodynamics of the Al–C–O system and properties of SiC–AlN–Al_2OC composites. *J. Eur. Ceram. Soc.* 1999, **19**, 2781–2787.
27. Qiu, C. and Metselaar, R., Phase relations in the aluminium carbide-aluminium nitride-aluminium oxide system. *J. Am. Ceram. Soc.* 1997, **80**(8), 2013–2020.
28. Yokokawa, H., Fujishige, M., Ujiie, S. and Dokiya, M., Phase relations associated with the aluminium blast furnace: aluminium oxycarbide melts and Al–C–X (X = Fe,Si) liquid alloys. *Metallurg. Transact. B* 1987, **18B**, 433–444.
29. *ASM Handbook, Vol 3, Alloy Phase Diagrams*, ed. H. Baker. ASM International, USA, 1992.